Electronic Supplementary Material (ESI) for Nanoscale.

SUPPLEMENTARY MATERIALS

Exosome-like silica nanoparticles: A novel ultrasound contrast agent for stem cell imaging

Fang Chen[a, b], Ming Ma[c], Junxin Wang[a], Fang Wang[d], Shixiong Chen[c], Eric Zhao[a], Anamik Jhunjhunwala[e], Sean Darmadi[a], Hangrong Chen[c], and Jesse V. Jokerst[a, b, *]

[a] Department of NanoEngineering, University of California, San Diego, 9500 Gilman Drive, La Jolla, CA 92093-0448, USA

[b] Materials Science and Engineering Program, University of California, San Diego, 9500 Gilman Drive, La Jolla, CA 92093-0418, USA

[c] State Key Laboratory of High Performance Ceramics and Superfine Microstructures, Shanghai Institute of Ceramics, Chinese Academy of Sciences, Shanghai, 200050, China

[d] Research Center for Bioengineering and Sensing Technology, University of Science and Technology Beijing, Beijing, 100083, China

[e] Department of Bioengineering, University of California, San Diego, 9500 Gilman Drive, La Jolla, CA 92093, USA

* Correspondence and requests for materials should be addressed to jjokerst@ucsd.edu.

Effect of size on the echogenicity of SSN

The echogenicity of five sizes of SSN (**Figure S2 A, B**) were measured at identical particle counts. The ultrasound intensity plateaus at 358 nm and declines when the size is 492 nm. The 358 nm SSN have ultrasound signal that is 64.8%, 69.5%, and 36.7% higher than the 260 nm particle and 18.9%, 20.5%, and 22.9% than the 492 nm particles at 1.25×10^{10}, 2.5×10^{10} and 5×10^{10} particles/ml, respectively ($p<0.0005$) (**Figure S2C**).

The ultrasound intensities of all five SSN increase with concentrations, but the linearity of ultrasound signal as a function of concentration is different. The R^2 values are 0.993, 0.999, 0.998, 0.952, and 0.932 for SSN for 60, 160, 260, 358, and 492 nm nanoparticles, respectively (**Figure S2 D**). The signal for the 358 nm and 492 nm particles at 5×10^{10} particles/ml drops compared to the linear fitting (**Figure S2 D**).

Effect of ordered 2D pores/channels on the ultrasound signals

We compared the ultrasound signal of similar sized SSN and MSN at identical particle-concentrations to determine the impact of the channels on acoustic signals. **Figure S3** shows the ultrasound images and processed data of SSN and MSN at the same particle-concentrations scanned at 40 MHz. As expected, both nanoparticles have increased signal as a function of concentration. The ultrasound signals of SSN at 2.5×10^{12}, 5.0×10^{12}, 1.0×10^{13} and 2.0×10^{13} particles/ml are 38%, 48%, 36% and 38% higher than that of MSN. Moreover, echogenicity of MSN was lower than that of SSN at all the measured concentrations. Porosity greatly increased the surface area, and the BET surface area of SSN is more than 10 times lower than that of MSN[39-41]. However, even though larger surface area may bear more air nanobubbles, the increased surface area in MSN didn't improve its echogenicity. Additionally, both particles were suspended in Millipore water without any degas procedures. Therefore, we may conclude that the echogenicity of silica nanoparticles is hardly attributed to air nanobubbles on their surfaces.

Instead, the negative effect of pores on the MSN may be attributed to two mechanisms. First, pores can decrease density of particles and thereafter reduce the impedance (production of density and velocity) mismatch between nanoparticles and their surroundings and eventually decrease the echogenicity of MSN. The BJH pore volume of ELS were determined empirically to be 1.79 cm^3/g, and that of MSN and MCF were reported to be 2.23 and 1.73 cm^3/g[42]. Correspondingly, the echogenicity of MCF and MSN was the highest and the lowest among three porous silica nanoparticles (**Figure 2J**). Additionally, the porosity of ELS is higher than MCF, and there are more ELS particles than MCF particles when their mass concentrations are the same. This may explain why echogenicity of the ELS was slightly lower than that of MCF with the same particle numbers, but it was higher than the echogenicity of MCF with the same mass concentrations (**Figure 2I, J**).

Second, the ordered and penetrating 2D channels on the MSN (**Figure S3**) may have decreased the effective backscattering interfaces and therefore weakened the echogenicity. Indeed, the echogenicity of porous MCF silica nanoparticles was increased

by introducing irregular external surfaces and a disordered 3D pore structure that creates multiple concave and convex structures (**Figure 2G**) to produce backscatter[27]. As shown in **Figure 2J**, the echogenicity of the MCF at 1.14×10^{11}, 2.28×10^{11}, 4.55×10^{11}, and 9.10×10^{11} particles/ml was 2.0-, 2.2-, 2.5-, 2.2-fold of that of SSN and 2.2-, 2.8-, 3.1, 3.3-fold of that of MSN. Moreover, the echogenicity of ELS may also be increased by incorporating disordered non-penetrating 2D pore structure as well as double convex/concave external surface as shown in the HRTEM imaging (**Figure 2H**).

Calculations for the density of MSN

$$\mathrm{N}v\rho = \mathrm{W} \qquad \text{Equation 1}$$

W – Total weight of nanoparticles; N – Total number of nanoparticles; v – Volume of one nanoparticle; ρ – Density of one nanoparticle.

$$\frac{N_1 v_1 \rho_1}{N_2 v_2 \rho_2} = \frac{W_1}{W_2} \qquad \text{Equation 2}$$

Both MSN and SSN are spheres. Therefore, when the total weight of SSN and MSN are the same, equation 2 can be converted to:

$$\frac{\rho_1}{\rho_2} = \frac{N_2}{N_1}\left(\frac{D_2}{D_1}\right)^3 \qquad \text{Equation 2}$$

NTA measurements indicated that there are $(76.9 \pm 3.2) \times 10^{10}$ and $(17.6 \pm 1.4) \times 10^{11}$ for 1 mg/ml of SSN and MSN. The average size of SSN and MSN are 160 nm and 154 nm. Therefore, the density of SSN is 2.04 times of MSN. It is noteworthy that equations 1-3 only fit for spheres.

Calculations for the nanoparticles/cell

NTA measurements indicated the number of particles in a 1 mg/mL sample was $(76.9 \pm 3.2) \times 10^{10}$, $(17.6 \pm 1.4) \times 10^{11}$, $(12.8 \pm 1.6) \times 10^{11}$, and $(13.7 \pm 0.3) \times 10^{11}$ particles/ml for SSN, MSN, MCF, and ELS, respectively. The Si content in SSN-, MSN-, MCF-, and ELS-labeled hMSCs were 0.40, 0.05, 0.75, and 1.11 ng/cell determined by ICP-OES. We converted the mass of Si to NPs first according to the NPs formula. Then, the number of NPs/cell was calculated by multiplying number of nanoparticles in 1 mg/ml solutions by mass of NPs per cell. The nanoparticles formulas and calculated nanoparticles/cell are listed in **Table S1**.

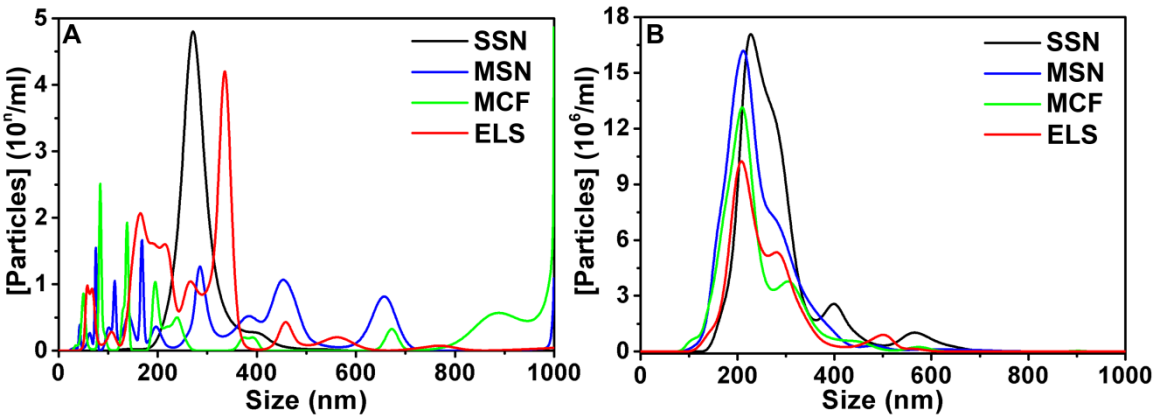

Figure S1. NTA size distributions of SSN, MSN, MCF, and ELS (A) before and (B) after sonication in water bath. The nanoparticles were dispersed in water. SSN slightly aggregated in water while the other three nanoparticles aggregated significantly. However, sonication can break down most aggregations of the MSN, MCF, and ELS. The hydrodynamic radii of SSN, MSN, MCF, and ELS are 246, 208, 202, and 208 nm respectively. (n=7 replicate experiments for SSN and n=6 replicate experiments for the other nanoparticles in panel A)

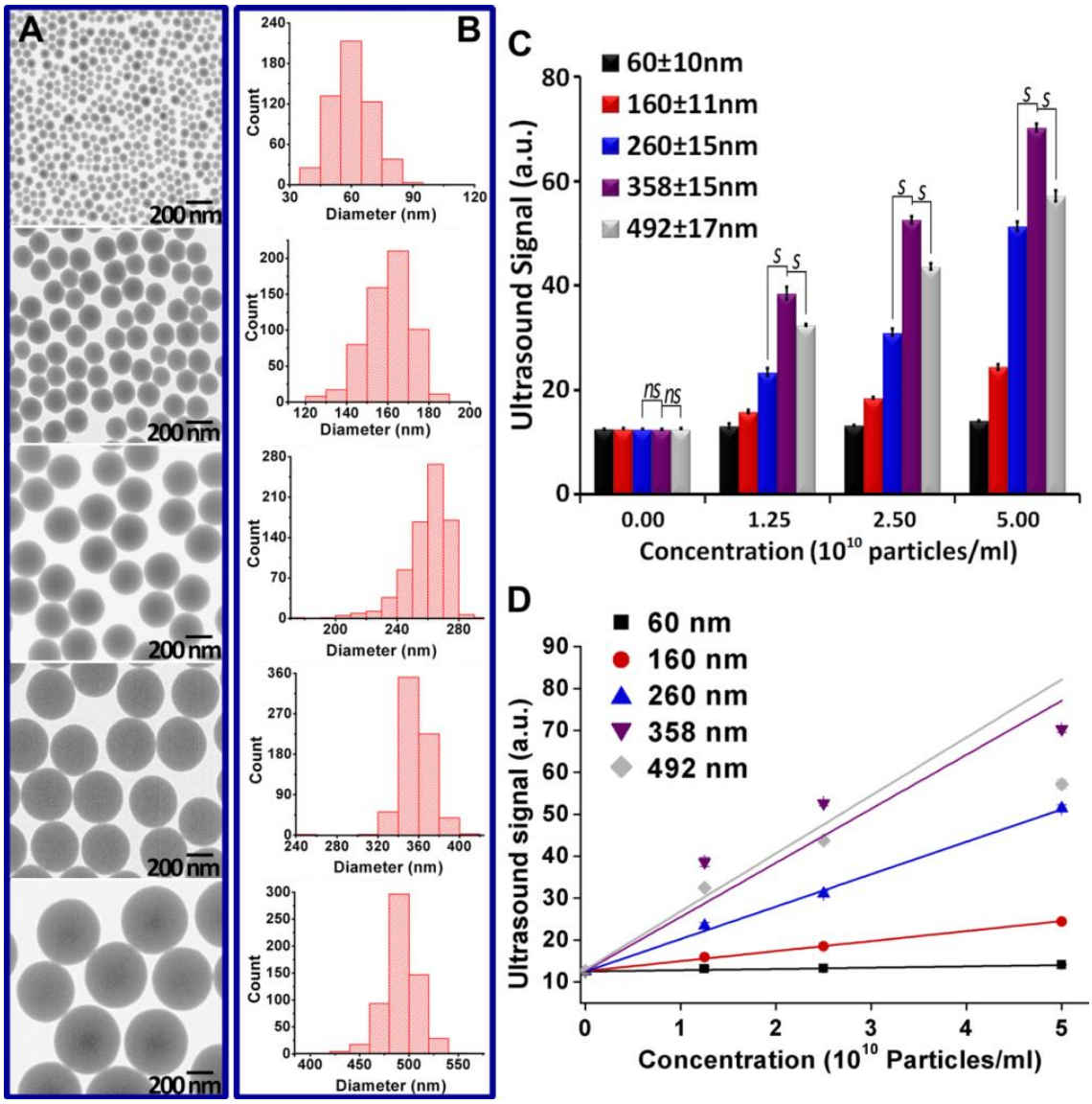

Figure S2. Ultrasound intensity as a function of size. (A) TEM images and (B) size distributions of SSNs with different sizes. (C) Ultrasound signal of SSN changes with size and particle concentration. The samples were scanned in an agarose phantom at 40 MHz. (ns: non-significant; s: significant). The ultrasound contrast increases as a function of SSN size, but then reaches a plateau at 358 nm and declines at 492 nm. The 358 nm SSN produce more signal than 260 nm and 492 nm nanoparticles ($p<0.0005$). Ultrasound intensities of all five SSN increase with particle-concentrations. (D) The linear relationship between ultrasound signal and particle-concentrations. The R-square values suggest that the most linear behavior occurs with particles smaller than 260 nm. Error bars represent the standard deviation of five replicate measurements. S: significant at $p<0.05$; NS: not significant.

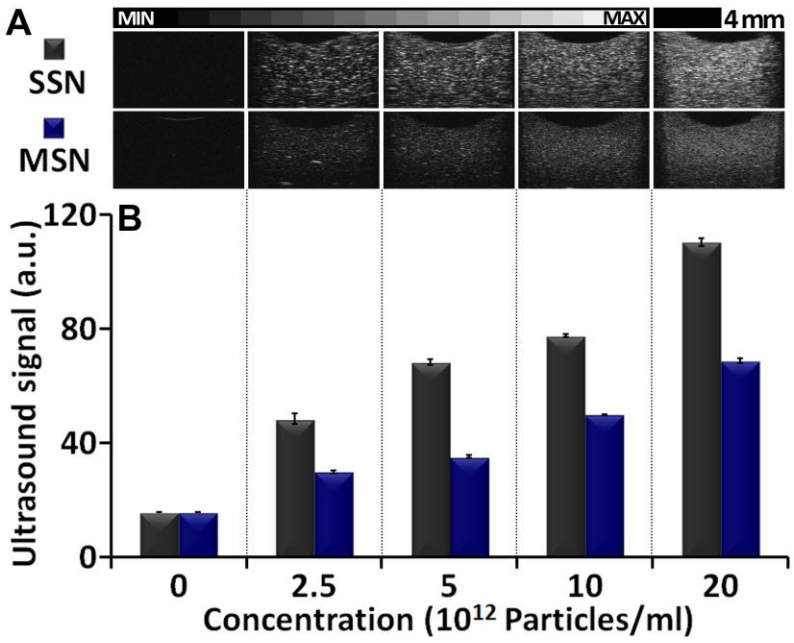

Figure S3. Effect of porosity on ultrasound signal. (A) Ultrasound images and (B) ultrasound intensity of SSN and MSN scanned at 40 MHz. Both the ultrasound images and image processing indicates that the nonporous SSN produce higher ultrasound contrast than porous MSN. Error bars represent the standard deviation of five replicate measurements.

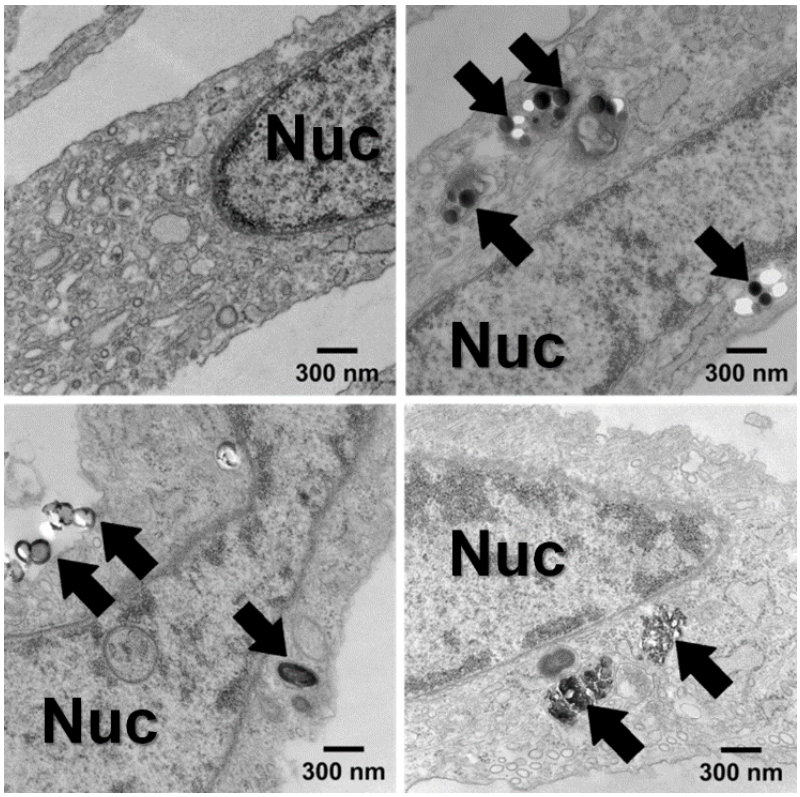

Figure S4. TEM images of (A) unlabeled hMSCs, (B) SSN-, (C) MSN-, and (D) MCF-labeled cells indicate all silica nanoparticles can be endocytosed by hMSCs without transfection reagents. All the cells were incubated under the same conditions except that different types of silica nanoparticles were used. Nuc stands for the nucleus, and the arrows indicate the silica nanoparticles.

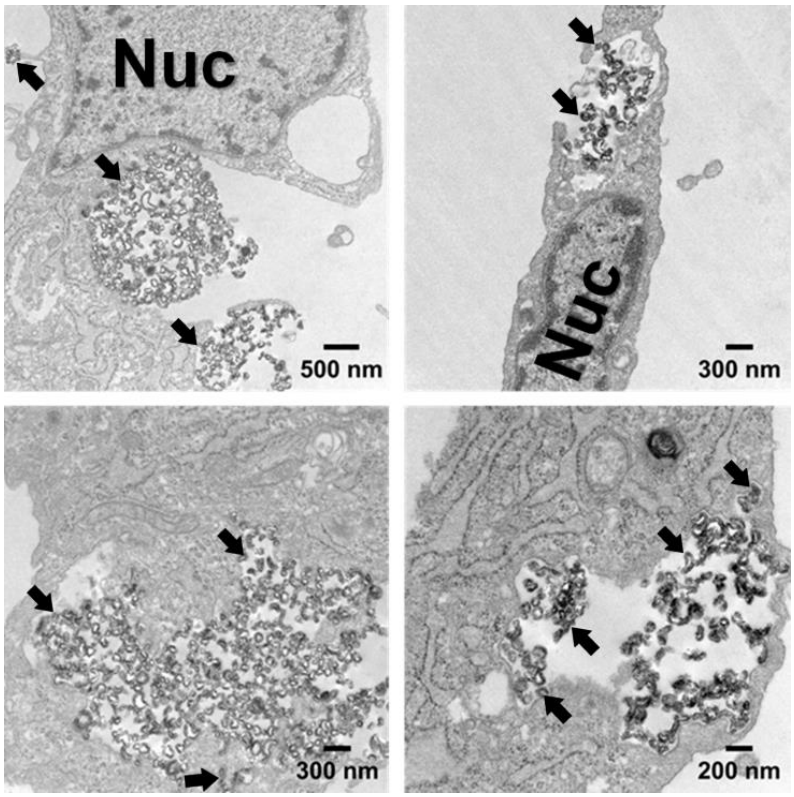

Figure S5. TEM images of ELS-labeled hMSCs indicate the endosomal uptake of the ELS nanoparticles. No transfection reagents were used. Nuc stands for the nucleus, and the arrows indicate the ELS nanoparticles.

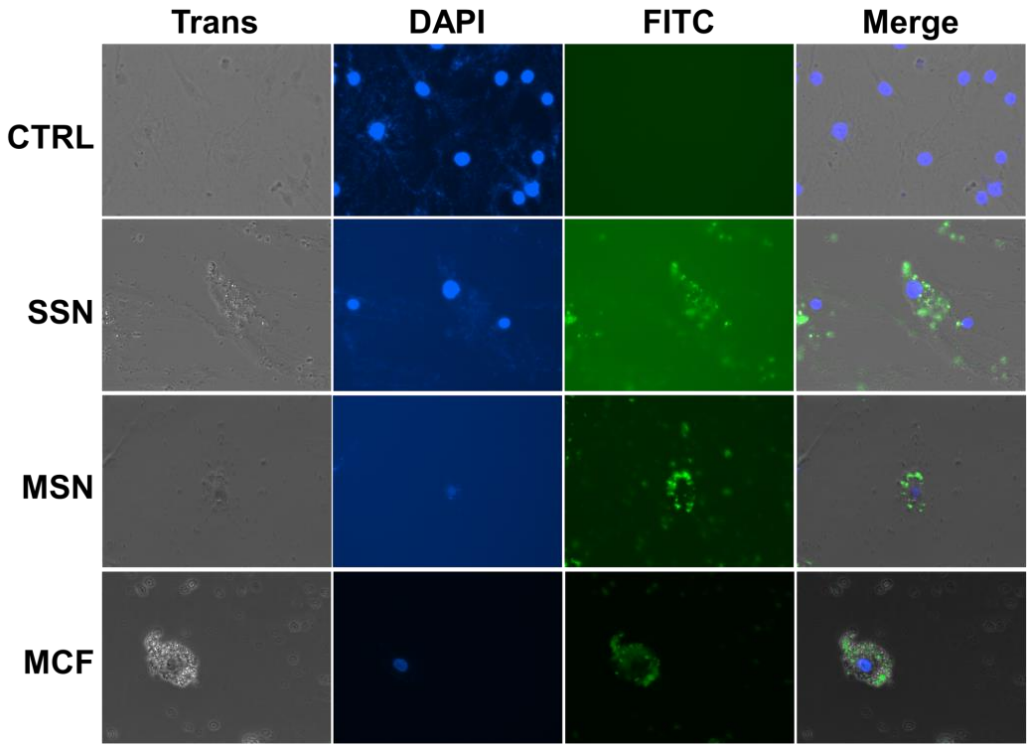

Figure S6. Epifluorescence images with hMSCs nucleus in blue and silica nanoparticles fluorescently tagged in green. The overlay images indicate most of the silica nanoparticles were specifically bound to the hMSCs.

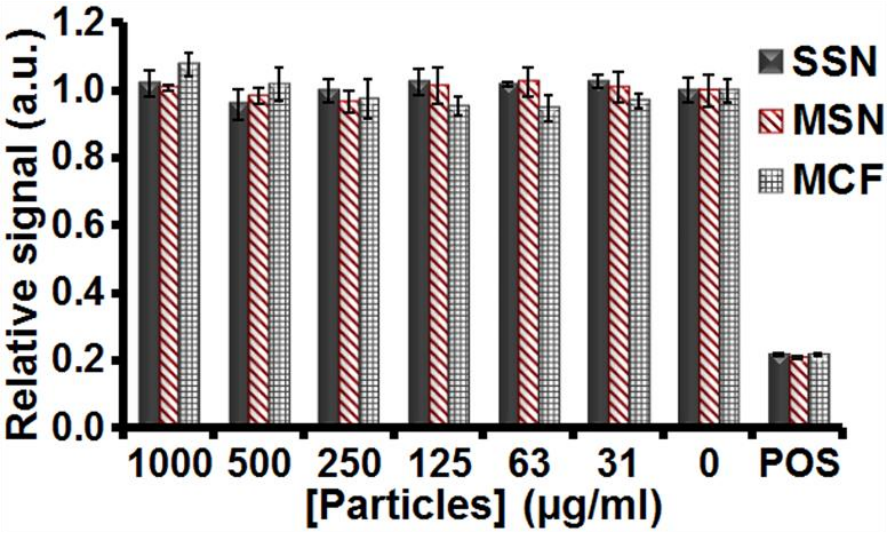

Figure S7. Cytotoxicity of SSN, MSN, and MCF. MTS assay indicated SSN, MSN, and MCF were non-toxic even up to 1 mg/mL.

Table S1. NTA and ICF-OES results, particles formulas, and calculated NPs/cell.

Particles	SSN	MSN	MCF	ELS
# of NPs in 1 mg/ml solutions ($\times 10^{10}$ NPs/ml)	76.9	176	128	137
Si (ng/cell)	0.40	0.05	0.75	1.11
NPs formula	SiO_2	SiO_2	SiO_2	$SiO_{1.5}C_{1.8}N_{0.2}$
Si:NPs	0.47	0.47	0.47	0.37
NPs (ng/cell)	0.86	0.11	1.60	3.02
# of NPs/cell (million)	0.66	0.19	2.05	4.14

Table S2. Zeta potential of silica nanoparticles before and after modification with (3-aminopropyl)triethoxysilane.

Zeta potential (mV)	Unmodified	Modified
SSN	-38.7 ± 1.30	3.65 ± 0.32
MSN	-32.0 ± 0.56	10.6 ± 0.51
MCF	-23.1 ± 2.67	21.2 ± 3.59

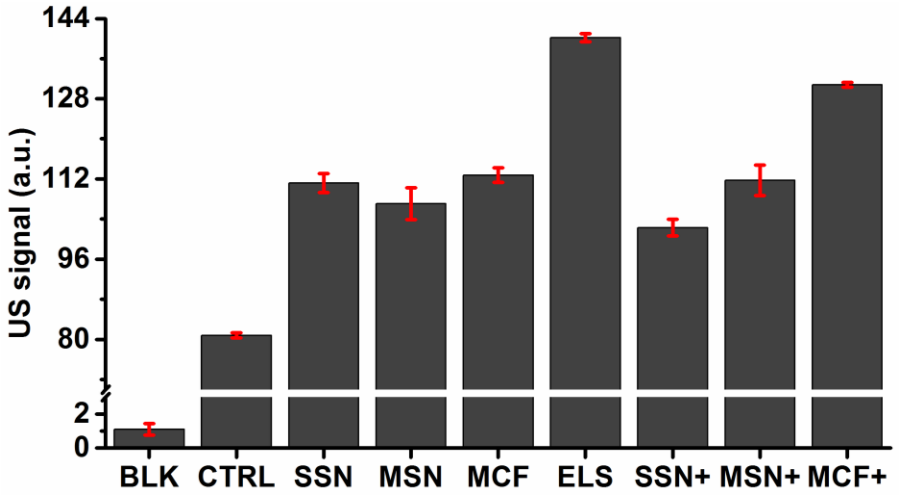

Figure S8. Ultrasound signal of unlabeled hMSCs (CTRL) and hMSCs labeled with SSN, MSN, MCF, ELS, amine modified SSN (SSN+), amine modified MSN (MSN+), and amine modified MCF (MCF+). The modification increased the cell labeling efficiency of MCF significantly and that of MSN slightly, while the same modification does not increase the cell labelling efficiency of SSN. However, the ELS still have the highest cell labelling efficiency even compared to the APTES-modified nanoparticles.

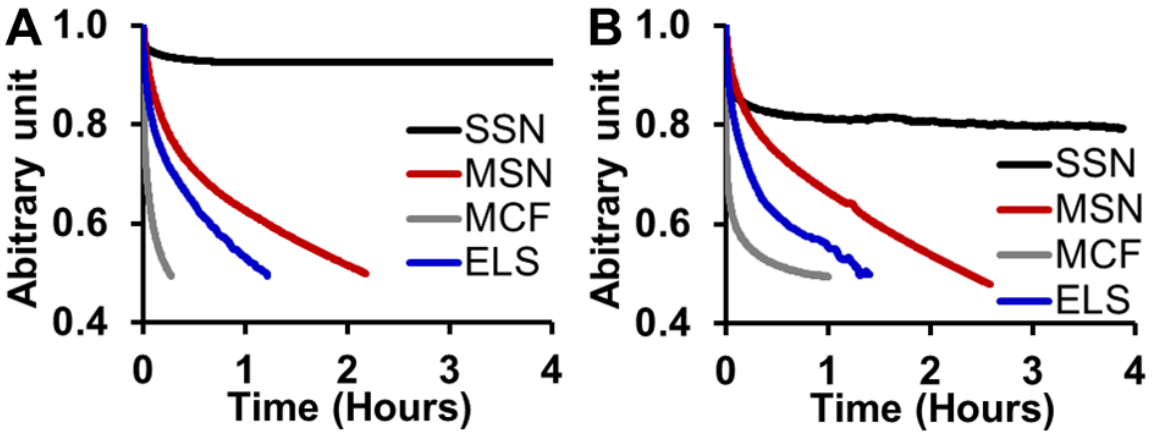

C

Time (Minutes)	SSN	MSN	MCF	ELS
WATER	> 600	130.5	15.5	72
25% FBS	> 240	142	47	78.5

Figure S9. Settling behavior of SSN, MSN, MCF, and ELS in (A) water and (B) 25% fetal bovine serum. (C) Time for the nanoparticles to settle by 50% in water and 25% FBS solutions as monitored by optical absorbance. The differences in the settling behavior of these nanoparticles are related to their zeta potential (**Table S2**) and heat treatment. The nanoparticles with higher absolute zeta potential tends to settle less and slowly. The calcination for MSN and MCF bring free silanol groups on their surfaces, which favor the aggregations. The hydrogen bond between amine groups within the frame and silanol group on the surface facilitate the aggregations for the ELS.